SN: 08/743,258
FD: 11-04-96
PATENTS-US--A8743258

S-78,079
Patent Application

ELECTRONUCLEAR ION FUSION IN AN ION CYCLOTRON RESONANCE REACTOR

RECEIVED
NOV 02 1998
OSTI

INVENTOR

DONALD F. COWGILL

930 Renada Place
San Ramon, California 94583

The correct
contract no. is
DE-AC04-76DP00789

DISCLAIMER

This report was prepared as an account of work sponsored by an agency of the United States Government. Neither the United States Government nor any agency thereof, nor any of their employees, make any warranty, express or implied, or assumes any legal liability or responsibility for the accuracy, completeness, or usefulness of any information, apparatus, product, or process disclosed, or represents that its use would not infringe privately owned rights. Reference herein to any specific commercial product, process, or service by trade name, trademark, manufacturer, or otherwise does not necessarily constitute or imply its endorsement, recommendation, or favoring by the United States Government or any agency thereof. The views and opinions of authors expressed herein do not necessarily state or reflect those of the United States Government or any agency thereof.

DISCLAIMER

Portions of this document may be illegible in electronic image products. Images are produced from the best available original document.

08/743,258 ✓	ELECTRONUCLEAR ION FUSION IN AN ION CYCLOTRON RESONANCE REACTOR	Donald F. Cowgill	DE-AC04-76DP00789

ELECTRONUCLEAR ION FUSION IN AN ION CYCLOTRON RESONANCE REACTOR

BACKGROUND OF THE INVENTION

The United States Government has rights in this invention pursuant to Contract No. DE-AC04-94AL85000 between the United States Department of Energy and Sandia Corporation.

Field of Invention

The present invention relates to electronuclear fusion of ions. More particularly, the present invention relates to a method and apparatus for producing energy through controlled nuclear fusion of ions by ion cyclotron resonance (ICR) acceleration.

Description of the Related Art

Conventional thermonuclear and inertial approaches seek to achieve fusion power by using brute force for containing, compressing, and heating a mixture of ions to fusion densities and energies. Electronuclear fusion occurs when energetic ions are directed on a target. For an idealized conventional beam-target interaction, for example, deuterons incident on solid tritium, about 1% of the energy expended for ion acceleration can be

returned as kinetic energy of the fusion reaction products, which in turn can be converted into electrical energy through thermal and direct conversion processes. The 99% energy loss of this conventional electronuclear approach results primarily from non-productive ion interactions with target electrons that rapidly retard the accelerated ions to energies that are not efficient for producing fusion reactions.

What is needed is an approach to generating nuclear fusion that reduces this energy loss by minimizing electronic stopping in the target region, that accommodates this reduced ion stopping by providing very long ion paths, and that causes accelerated ions to interact with target nuclei only at energies corresponding to a peak in the fusion yield. That is, an approach is needed that creates nuclear fusion of ions stored in an ion trap reactor, that maintains control of and corrects individual energetic-ion orbits to prevent ion detrapping, that localizes target ions in the ion reactor, and that forces unlike ions to interact repeatedly at the optimum energy until fusion occurs.

SUMMARY OF THE INVENTION

The present invention provides a method and apparatus that reduces the electronic energy loss by minimizing electronic stopping in the target region and forces accelerated ions to continually interact with target nuclei only at energies corresponding to the peak in the fusion yield. By doing so, the total energy input required to produce fusion for the present invention is kept lower than the energy released by the fusion reaction producing a positive energy gain. Further, the present invention uses efficient methods for ion

acceleration, ion orbit control, and target ion generation, which minimizes peripheral energy requirements and results in a source of power.

The two fusing species of ions of the present invention are controlled separately. This differs from conventional thermonuclear approaches where energy transfer times are such that all ions, along with electrons, are compressed and heated together. In either case, each energetic ion represents an investment of energy, that is, an acceleration, and it is important to prevent its loss. In the present invention, the density of energetic ions can be kept low for minimizing their interaction and for increasing their lifetime τ in the trap. The present invention energizes ions in directed orbits and provides corrections to orbit deviations resulting from the numerous small-angle scattering events with target ions. For the non-energized target species, a high density n is required, but with little concern for target ion detrapping. Separation of the density and lifetime requirements simplifies achievement of the $n\tau$-criterion for high probability of fusion, when compared with conventional thermonuclear approaches where n and τ pertain to both ion species simultaneously.

In the present invention, the non-resonant target ion species is produced near the outer wall of the reactor (or some other localized interaction region). In the preferred embodiment, it is generated by ion-induced desorption through the interaction of accelerated ions with a gas layer adsorbed on the wall. By doing so, a high target ion density is produced in the desired location, with automatic feedback control of the target ion production. Alternatively, with appropriate control, the target species ions can be injected into the trap from an external source.

In this regard, the present invention provides a method and apparatus, an ion cyclotron resonance reactor, for generating the fusion environment. The reactor, an evacuated Penning-type ion trap, includes a cylindrical housing having an axial axis, an internal surface, and first and second end plates. First and second end plates are electrically charged to repel the ions and are respectively located at the first and second ends of the cylindrical housing. A strong, uniform magnetic field oriented along the axial axis of the cylindrical housing confines trapped ions in axially-oriented helical orbits. A gas layer of the target species is adsorbed or cryo-condensed on the internal surface of the cylindrical housing. This layer can be replenished continuously or periodically, as needed. A significant fraction of this gas layer is desorbed as low energy ions, forming a thin plasma layer of first (target) ions trapped near the surface by the magnetic field and the first and second end plates. These first ions are desorbed by the interaction of second (energetic) ions with the adsorbed gas layer. The second ions are unlike the first ions, but have the same charge, and are introduced on the axis of the cylindrical housing by injection from an ionizer. A transverse radio frequency (RF) field resonantly accelerates the injected second ions at their ion cyclotron resonance (ICR) frequency in expanding helical orbits to an energy level that is ideal for nuclear fusion with the trapped first ions. By balancing the RF energy input to the second ions with their rate of tangential energy loss in the layer of first ions, the trapped first and second ions are forced to interact repeatedly at the ideal energy.

More specifically, the energy level E_0 to which the second ions are resonantly accelerated corresponds to a peak of the fusion Q power amplication factor, for fusion of

the second ions with the first ions, and results in a fusion reaction having unity probability when

$$n_t \tau_i = 1/(\sigma v)_0 , \quad (1)$$

where, n_t equals the density of the first ions, τ_i equals the mean lifetime of the second ions, σ is the fusion reaction cross-section of the second ions at E_0 with the first ions, and v, the tangential velocity of the second ions, is defined by

$$v = 2\pi R f_0 , \quad (2)$$

where R is the radius of the cylindrical housing and f_0 is the cyclotron resonance frequency of the second ions.

According to one embodiment of the invention, the first ions are deuterons and the second ions are tritons. According to another embodiment of the invention the first ions are tritons and the second ions are deuterons. In yet another embodiment of the invention, the first ions are deuteron ions and the second ions are ^{3}He ions. In still another embodiment, the first ions are ^{3}He ions and the second ions are deuteron ions.

The anticipated output of the present invention is in the watt-to-kilowatt range, but possibly much greater. Its main potential for use is for powering homes, autos, etc., individually. The present invention also may be used for remote or space applications. Many such reactors may be assembled to form a large power plant or be used in a

distributed power system, reducing power transmission costs. Sufficient tritium and deuterium for a 10-year life is easily sealed within the small reactor and which could be refilled at a reconditioning station. The trap and acceleration scheme are simple, much less expensive, and potentially much more cost effective than proposed large, complicated, magnetic and inertial confinement thermonuclear machines.

BRIEF DESCRIPTION OF THE DRAWINGS

The present invention is illustrated by way of example and not limitation in the accompanying figures in which like reference numerals indicate similar elements and in which:

Figure 1 is a graph showing the relative magnitudes of ion stopping components for t^+ ions in deuterium;

Figure 2 is a graph showing beam target (B-T) fusion Qs for a TD reaction for different stopping components;

Figure 3 shows fusion Q curves for screened and bare nucleus deuterium-tritium (DT) and tritium-deuterium (TD) reactions;

Figure 4 shows fusion Q curves for screened and bare nucleus deuterium-helium-3 (D^3He) and helium-3-deuterium (^3HeD) reactions;

Figures 5A and 5B show an ICR reactor according to the present invention; and

Figure 6 is a graph showing the calculated power production for an exemplary ICR reactor according to the present invention having a 2.54 cm radius and a 20 cm length with target ion densities in the range 10^{13} - 10^{15} cm^{-3}.

DETAILED DESCRIPTION OF THE PREFERRED EMBODIMENTS

The present invention uses an evacuated Penning ion trap for generating long ion paths and lifetimes and for minimizing wasteful energy loss to electronic excitation processes. To achieve this, energetic ions are produced by ion cyclotron resonance (ICR), while target ions are generated by ion sputtering/desorption. Trap potentials and dissipative damping are used for controlling scattering effects on both the ion orbits and target ion distribution.

According to the present invention, the energetic and target ions are forced to interact only at an optimum energy condition for fusion which is maintained until fusion occurs. Attaining the condition for high fusion probability for a target ion density n_t and incident ion lifetime τ_i, that is,

$$n_t \, \tau_i = 1/(\sigma v)_0 \, , \tag{3}$$

where $(\sigma v)_0$ is the peak fusion reactivity, produces fusion power amplification factors of $Q > 1$ for both deuterium-tritium (DT) and deuterium-helium-3 (D^3He) reactions. The net power output for a "beer can" size reactor according to the present invention with target ion densities about 10^{14} cm^{-3} is in the watt-to-kilowatt range depending upon specific parameter selection.

In contrast to conventional thermonuclear and inertial approaches, the present invention creates repeated energetic interactions only between unlike ions and does so only at the ideal energy for fusion. Energy is supplied to ions in a "directed" fashion, thus avoiding wasting energy in translational degrees of freedom not contributing to a fusion

reaction. However, when the directed energy is transferred among the ions through scattering interactions, this scattering contributes an energy loss not experienced with thermonuclear approaches. The scattering interactions limit the power amplification or fusion Q, the ratio of energy output to the total energy supplied to the ion, to be less than the thermonuclear limit. If during scattering, though, the directed ion energy loss is compensated by a small continuous acceleration, e.g., by ICR, then the directed ion energy can theoretically be held constant until a fusion reaction occurs.

The fusion yield Y, or probability of a fusion reaction, for an ion travelling with energy E to E + dE in a target is $dy = (\sigma/s)dE$, where $\sigma(E)$ is the fusion reaction cross-section and s(E) is the ion stopping power of the target. Both $\sigma(E)$ and s(E) depend strongly on ion energy. For an ion having energy E_0 that is incident on a target in which the ion is stopped, the total yield Y is calculated by integrating (σ/s) over energy from E_0 to zero. The energy produced by the ion is the product of the yield Y and the reaction energy ΔMc^2, the energy equivalent of the mass difference between the initial and final nuclear products. Thus, for the decelerating ion, $Q = Y(\Delta Mc^2)/E_0$. It follows that the beam-target (B-T) expression for Q is:

$$Q_{B\text{-}T}(E_0, 0) = [(\Delta Mc^2)/E_0] \int_0^{E_0} (\sigma/s) dE. \qquad (4)$$

As mentioned, if during the interaction with the target, the ion energy loss is compensated by a small continuous acceleration, for example, by ICR, then the ion energy can theoretically be held constant at E_0 until a fusion reaction occurs. In such a situation, the

yield Y is unity. That is, $Y = (\sigma/s)_0 \Delta E = 1$, where ΔE is the additional energy supplied to the ion and $(\sigma/s)_0$ is the value of (σ/s) at E_0. The fusion Q then becomes

$$Q_{ICR}(E_0) = (\Delta M)c^2 / [E_0 + 1/(\sigma/s)_0]. \quad (5)$$

An interaction with Q = 1, that is, at breakeven, consumes as much energy as is produced, while for Q > 1, net energy is produced.

In the energy range of interest, the most efficient fusion reaction is deuterium incident on tritium (DT), or reversed as a tritium incident on deuterium (TD) reaction, both symbolized by

$$D + T \rightarrow n + {}^4He + 17.6\ MeV, \quad (6)$$

DTC 10/4/96

where the reaction energy $\Delta Mc^2 = 17.6$ MeV. Other reactions of potential interest include DD and D^3He reactions:

$$D + D \rightarrow n + {}^3He + 3.25\ MeV, \quad (7)$$

$$D + D \rightarrow H + T + 3.98\ MeV, \quad (8)$$

$$D + {}^3He \rightarrow H + {}^4He + 18.3\ MeV. \quad (9)$$

The cross-sections for these reactions have been examined by others and are summarized by H. Liskien and A. Paulson in Nuclear Data Tables 11, pp. 569-619, 1973, and by A. Peres in Journal of Applied Physics 50, p. 5569, 1979, both of which are incorporated by reference herein.

For a given E_0 in either case, DT or TD, fusion Q is maximized by minimizing the ion stopping s, the energy loss of the ion per unit thickness of target traversed. The stopping s is determined by the sum of inelastic electronic excitation s_e and elastic nuclear scattering s_n components,

$$s = \eta s_e + s_n . \tag{10}$$

Each term of the stopping s is treated as separable because a recoiling target nucleus can be considered to be unconnected from other nuclei during the passage of the ion. The factor η is included for accommodating an electrically charged target containing an excess or a deficient concentration of electrons. For an electronically neutral target, $\eta = 1$. There is good theoretical understanding of these stopping components at both high and low energies. Electronic stopping as an interaction with a density-averaged free electron gas has been formulated by J. Lindhard, K. Dan. Vidensk. Selck. Mat. Fys. Medd. 28 (8), 1954, and J. Lindhard and A. Winther, ibid. 34(4), 1964, incorporated by reference herein. Nuclear stopping is usually treated as simple kinetic scattering of two screened particles. Both contributions to stopping s for hydrogen and helium ions in many materials are examined by J.F. Ziegler, Nucl. Instr. Meth 168, p. 17, 1980, incorporated by reference herein, where it is concluded that $s_n << s_e$ in the energy range of interest. For

s_n, Ziegler uses the theoretical value of the Lindhard, Scharf and Schiott (LSS) formula represented by

$$8s_n = A \ln (1 + \epsilon)/(\epsilon + 0.10718\epsilon^{0.37544}), \quad (11)$$

where ϵ is a reduced energy. This expression has been shown by Wilson et al., Phys. Rev. 15B, p. 2458, 1954, to produce a good fit for existing nuclear stopping data. The constant A and the factor ϵ/E for the reactions discussed above are listed in Table I where fusion Qs and resonance energies for ions experiencing nuclear stopping only are shown. The Q-spread shown in Table I is based on bare-coulomb ion stopping at one extreme to screened-coulomb ion stopping at the other extreme. Experimental data for s_e of H in the elements has been compiled by H.H. Anderson and J.F. Ziegler, Hydrogen Stopping Powers and Ranges in All Elements, Volume 3, Pergamon, New York, 1977, and incorporated by reference herein. A simple analytic formula is used by Anderson and Ziegler for bridging the theoretical descriptions at high and low energy and for producing good fits to the data at intermediate energies. A similar treatment of the stopping for He ions is given by J.F. Ziegler and W.K. Chu, Atomic Data and Nuclear Data Tables 13, p. 463, 1974, and incorporated by reference herein.

Figure 1 shows the relative magnitudes of s_n and s_e stopping components for t^+ ions in deuterium. Curve 10 represents the relative magnitude of s_e and curves 11 and 12 represent the relative magnitudes of bare-coulomb stopping and screened-coulomb stopping, respectively. For condensed or gaseous D_2 or for neutral plasmas ($\eta = 1$), s is strongly dominated by s_e. However, Figure 1 shows that reducing the relative electron

DFC 10/4/96

density η can produce a large reduction in the ion stopping. By Eq. (4), elimination of the electronic stopping component can increase the yield, or fusion Q, by as much as 10^3.

TABLE I

Reaction	DT	TD	DD	D^3He	^3HeD
ϵ/E	13.794	9.208	11.501	6.064	4.048
A	1.198	1.794	1.496	2.106	3.155
$Q_{BT}(E_0,0)$	4.6-6.8	3.1-4.6	< 1	1.0-2.0	0.6-1.3
@ E_0(keV)	275	400	> 10^4	1600	2400
$Q_{ICR}(E_0)$	6.8-10.1	4.6-9.7	< 1	1.3-2.7	0.9-1.8
@ E_0(keV)	131	196	3000	800	1200
$n_t\tau_a(10^{15}$ $cm^{-3}s)$	0.61	0.61	2.86	1.84	1.84

Significant changes in the relative electron density, however, also affects the screening of the coulomb interaction responsible for s_n. The extent of this effect can be seen by evaluating nuclear stopping for unscreened coulomb scattering. J.B. Marion and F.C. Young disclose in Nuclear Reaction Analysis (North-Holland Amsterdam, 1968), which is incorporated by reference herein, that the energy loss of a scattered ion can be written as

$$E_0 - E = E_0 \, [2m_i \, m_t/(m_i + m_t)^2 \,](1 - \cos \theta_c \,), \qquad (12)$$

where m_i and m_t are the incident and target ion masses, respectively, and θ_c is the scattering angle in the center-of-mass system. The scattering angle is related to the impact parameter b by

$$\tan(\theta_c/2) = e_i\, e_t /[8\pi\epsilon_0\, (m_r/m_i)E_0\, b], \tag{13}$$

where e_i and e_t are the incident and target charges, ϵ_0 is the permittivity of free space, and $m_r = m_i m_t/(m_i + m_t)$. The average nuclear stopping produced by the scattering interaction is

$$s_c = \int_0^{b_{max}} (E_0 - E)\, 2\pi b db, \tag{14}$$

DFC 10/4/96

where maximum impact parameter is determined by the spacing of the target nuclei. For a target with ion density n_t, $b_{max} \approx n_t^{-1/3}$. Combining Eqs. (10)-(12) and integrating yields

DFC 10/4/96

$$s_c = 4\pi E_0\, (m_r^2/(m_i\, m_t)\lambda^2 \ln [1 + (1/\lambda n_t^{1/3})^2\,], \tag{15}$$

where

$$\lambda = e_i\, e_t /[8\pi\epsilon_0\, (m_r/m_i)E_0\,]. \tag{16}$$

Thus, the ion stopping by unscreened coulomb scattering varies approximately as $m_i/m_t E_0$ and depends weakly on n_t. Since $\sigma = \sigma(E_0/m_i)$, this means σ/s_c is slightly larger when $m_i < m_t$. The stopping given by Eq. (15) with $n_t = 10^{14}$ ions/cm^3 is also plotted in Figure 1. It shows that without the screening effect of the electrons, the nuclear stopping is slightly larger.

There is reason to believe that the ion stopping due to electrons in a plasma may not be as large as described above. Lindhard's theory of electronic stopping, which gives rise to the s_e curve 10 in Figure 1, is based on ion interactions with a free electron gas at zero temperature and predicts that when the velocity of the ion is less than the Fermi velocity, the electronic stopping drops. While curve 10 is appropriate for solids where the Fermi energy is a few eV, electrons trapped in a target plasma can reach somewhat higher energies; hence, their stopping may be less. A reduced electronic stopping is consistent with observed ranges of the ions injected into neutral tokamak plasmas, such as disclosed by W.M. Stacey, Jr. in chapter 1 of Fusion: An Introduction to the Physics and Technology of Magnetic Confinement Fusion, Wiley-Interscience, New York, 1984, incorporated by reference herein. Thus, if the target ion density is high enough to produce significant electron trapping in its positive space charge, the ion stopping may be better described by a screened coulomb interaction along with a weaker electronic effect. Heating the electrons to a few keV may result in the screened nuclear stopping alone. For the exemplary fusion Q's evaluated below, results are provided for both bare coulomb stopping and screened nuclear stopping. The Qs for the screened nuclear stopping case are considered the maximum Qs that can result.

DFE 10/4/96

Figure 2 shows beam target (B-T) fusion Qs determined by Eq. (4) for a TD reaction with the stopping given by $s_e + s_n$, s_n, and s_c. For T incident on solid deuterium, the maximum Q is about 1%, as shown by curve 20 with $s = s_e + s_n$. Elimination of all electrons in the target region increases the fusion Q by a factor of 330, producing $Q_{B\text{-}T} = 3.1$ (curve 21). For a DT reaction, $Q_{B\text{-}T} = 4.6$ (curve 22). Curves 20-22 are

nearly flat for energies beyond about 100 keV/amu. The addition of energetic electrons may increase these Qs, as described above, if the electrons produce significant nuclear screening and little stopping. The maximum increase is about 50%, as shown by curve 22 with $s = s_n$. Since $Q_{B\text{-}T} > 1$ for these reactions, it follows that net energy can be produced by simply introducing energetic ions into an efficient trap containing the target ion species. Fusion Q curves obtained for deuterium-tritium (DT) reactions using the ICR approach with ionized targets are shown in Figure 3, where the abscissa is ion energy measured in keV and the ordinate is fusion Q, that is, the ratio of energy output to the total energy supplied to an ion. The curves of Figure 3 peak at an "ideal" or resonant ion energy. The maximum Q, which occurs for D on T (DT), is $Q_{ICR} = 6.8$ without screening (curve 30) and $Q_{ICR} = 10.1$ with screening (curve 31). In either case, with or without screening, the fusion Q is greater than 1. For T on D (TD) the maximum fusion Qs drop to 4.6 and 9.7 for bare nuclei (curve 32) and with screening (curve 33), respectively. Similar conclusions regarding the energy gain for two component DT plasmas have been reached by J.M. Dawson and others (G.H. Miley and H.H. Towner in NBS 425, Nuclear Cross Sections and Technology, Vol. 2, Washington D.C., 1975, p. 719), incorporated by reference herein.

Broad ICR resonances also occur for D^3He and ^3HeD interactions and are shown in Figure 4 where the abscissa is ion energy measured in keV and the ordinate is fusion Q. The maximum Q for D on ^3He (D^3He) is $Q_{ICF} = 1.3$ without screening (curve 40) and $Q_{ICF} = 2.7$ with screening (curve 41). For ^3He on D (^3HeD), the fusion Qs drop to 0.9 and 1.7 for bare nuclei (curve 42) and screening (curve 43), respectively. Although the

reactions shown in Figure 4 generally produce smaller Q values, both bare and screened D^3He reactions and a screened ^3HeD reaction have a power amplification of $Q > 1$. All of these reactions produce no nuclear activation products and are compatible with efficient direct conversion to electrical energy.

Figures 5A and 5B show an ICR reactor 50 according to the present invention. Although this description is given specifically for a TD reactor, the overall concept also is viable for a DT, D^3He, and ^3HeD reactors, although the D^3He, and ^3HeD reactors are less efficient than the DT and TD reactors. Reactor 50 includes a Penning-type positive ion trap 51 having an evacuated concentric cylindrical housing 52 having a radius R with Penning traps plates 53 and 54, which are shown as being planar, but can be non-planar. DFC 10/4/96 Plates 53 and 54 are positively charged by a source (not shown) in a well-known manner. Solenoid 55 generates a strong uniform magnetic field H_o that is oriented along an axial axis 56 of ion trap 51. Thermal ionizer 57 is coupled to plate 53 and introduces tritium ions (t^+ or tritons) along axial axis 56 of the ion trap. A second ionizer can be coupled to plate 54 for introducing tritium ions along axis 56 from an opposite direction. Other well-known methods of producing tritium ions, such as in-situ ionization, may also be used. A liquid nitrogen layer 63 is applied to the outer surface of housing 52 in a well-known manner.

The tritons circulate in helical orbits 59 about the magnetic field lines of H_o and are trapped between the repulsive end plates 53 and 54. The tritons are resonantly accelerated by an imposed RF field E_{rf} at the t^+ ICR frequency by RF plates 60 in a well-known manner. The triton orbits increase in radius, similar to the ion behavior in an Omegatron

partial pressure analyzer as disclosed by D. Albert and R.S. Buritz in "Ultra-High Vacuum. II. Limiting Factors on the Attainment of Very Low Pressures", J. Appl. Phys., 25, 1954, pp. 202-209, and by S. Dushman, Scientific Foundations of Vacuum Technique, 2nd Edition, J. Wiley and Sons, New York, 1966, pp. 342-349, both of which are incorporated by reference herein. The triton orbits increase in radius until the tritons interact, at grazing angles, with a deuterium gas layer 61 that is adsorbed or cryo-condensed on the internal surface of the concentric cylindrical housing 52 by the liquid nitrogen layer 63. Sputtered or desorbed deuterium atoms and molecules, deuterons (d^+) and molecular ions (e.g., d_2^+), and electrons are ejected from gas layer 61. The deuterons are non-resonant with the imposed RF field and are trapped in small spirals near the surface of housing 52 by the axial magnetic field H_0 and the electrostatic repulsion of plates 53 and 54. The deuterons form a weak plasma target layer 62 adjacent to the internal surface of housing 52. Balancing the triton's ICR energy input with its energy loss due to nuclear stopping in the d^+ layer and any remaining electronic stopping forces the energetic t^+ ions to continuously interact with the d^+ ion plasma at a single energy. This energy is chosen to correspond to the peak of the fusion Q by proper selection of radius R of cylindrical housing ~~32~~ 52 as described below.

DFE 10/4/96

Ejected electrons, being more mobile than the deuterons, rapidly escape to the positively-charged end plates 53 and 54 and the thin target layer 62 that forms over the internal surface of housing 52 becomes enriched with deuterons and depleted of electrons. Trapped molecular ions are eventually dissociated by interaction with energetic t^+ ions. Sputtered atoms, molecules and deuterons that become neutralized are re-adsorbed (or

recondensed) back into the gas layer 61, restoring the deuterium reservoir. Helium produced by tritium decay and the fusion reaction is evacuated through appropriate ports 58 that maintain ultra high vacuum (UHV) conditions within reactor 50. ~~The partial pressure of a solid deuterium reservoir at 4.2 K for the exemplary reactor configuration described is less than 10^{-10} torr.~~ DFC 10/4/96

The energy loss per cycle experienced by a triton in the d^+ layer is $\delta E_t = 2\pi R s n_d$, where n_d is the deuteron density in the layer. Holding the triton energy at the fusion resonance condition until the triton reacts requires a total average energy input of DFC 10/4/96 $\Delta E = 1/(\sigma/s)_0$. The average number of cycles for a triton is $\Delta E/\delta E_t = 1/2\pi R n_d \sigma_0$. Equating this with $f_0\tau_t$, where τ_t is the mean lifetime of a triton, generates a condition relating n_d and τ_t. Inserting the tangential triton velocity $v_t = 2\pi R f_0$ produces the criterion for a fusion reaction with unity probability:

$$n_t \tau_i = 1/(\sigma v)_0 . \qquad (17)$$

The subscripts in Eq. (17) have been changed to reflect the incident (i) ion and the target (t) ion. This $n\tau$ product is listed for each reaction in Table I and depends only on the relative velocity v of the ions, making its value independent of which ion is accelerated. For the TD reaction, this criterion means that the average triton will live 6 sec in a target layer having a density of 10^{14} d^+/cm^3. By the same argument, this lifetime is a requirement for producing the computed Q_{ICR}. If the triton is detrapped earlier, the Q will suffer a proportionate reduction. DFC 10/4/96

The $n\tau$ requirement is similar to that computed for a thermonuclear fusion reaction having $Q \approx 15$ and $n\tau_E \approx 2 \times 10^{14}$ s/cm^3, where τ_E is the energy confinement time. Although the DT reactivity at resonance $(\sigma v)_0 = 1.64 \times 10^{-15}$ cm^3/s is about 60% larger than the peak thermonuclear ~~reacting~~ reactivity $\langle \sigma v \rangle$ averaged over a Maxwellian energy distribution, the $n\tau$ requirement given by Eq. (17) is about three times higher, that is, $n_i\tau_i = 6 \times 10^{14}$ s/cm^3. This difference is due to energy lost by nuclear scattering, which occurs in the ICR case, but not in a tokamak. In a tokamak, the scattered energy remains useful as plasma heat. Although the $n\tau$ requirement is increased by a factor of three for the ICR approach of the present invention, the two parameters are for two different ion populations. Thus, parameters may be optimized separately, subject to coulomb scattering limitations, giving the ICR approach of the present invention greater flexibility for achieving the $n\tau$ requirement than conventional fusion approaches.

DFC 10/4/96

There appears to be no lower limit to the incident ion density required to produce fusion ($Q>1$) in an efficient ion trap. A single triton introduced on axis 56 interacts with the deuterium reservoir at high energy where its probability of neutralization is small. Little is known about the sputtering of adsorbed D monolayers or the self-sputtering of solid hydrogen, but at the higher energies of interest, it is expected to be much greater than unity and to occur primarily as ions. If the trapping lifetimes of t^+ and d^+ are long, repeated wall interactions will occur until the triton has built up a target layer of sufficient density to prevent it from reaching the wall. At this point, the layer is maintained by only an occasional t^+-wall interaction for accommodating the d^+ loss. Thus, at low t^+ concentration, the triton burnup is quite efficient, leaving little residual tritium gas to

DFC 10/4/96

contaminate the reactor. However, at low t^+ concentration, the power production will also be small.

For higher t^+ and d^+ densities, scattering causes the trapping lifetimes to decrease, reducing the overall reactor efficiency. The target layer may be completely replenished by the sputtering from energetic scattered deuterons and fusion reaction products. If the fraction of sputtered neutrals is high, it may be desirable to introduce the tritium as a dilution to the deuterium charge.

The maximum deuteron density that can be obtained in a reversed Penning trap when the d^+ ions are introduced in the manner shown in Figure 5A is unknown. Ion trapping in this configuration has been investigated where the aim was to obtain long ion lifetimes as disclosed in an article entitled "Confinement of Ions for Collision Studies", reviewed by J.B. Hasted in Physics of Ion-Ion and Electron-Ion Collisions, Brouillard and McGowns, editors, Plenum, New York, 1983, p. 484, and incorporated by reference herein. To lengthen ion lifetimes, the effects of fringing fields were disclosed as being reduced by making both the cylinder and end plates in the shapes of hyperboloids of revolution. In a background pressure of 10^{-10} torr, ion lifetimes of 300 seconds were observed for ion densities of 10^6 cm^{-3}. Using space-charge assistance, ion densities of 10^9 cm^{-3} were readily obtained. In both cases, however, the ions were introduced by gas ionization in a low pressure discharge, where the ion density was limited by scattering of the background gas. Here typical gas densities were 10^{13} cm^{-3}. Significantly greater ion densities should result when the limitation caused by background gas scattering is removed. As the ion density increases, electrons will be trapped in the positive space charge. As

previously discussed, these trapped electrons produce, at most, only a small scattering loss. Deuteron densities obtained in a "minimum-B" magnetic trap configuration reach 10^{14} d^+/cm^3, where deuterons are lost by scattering into a loss cone defined by the field pinch. This particular loss mechanism is absent in the trap configuration of the present invention.

A measure of ion confinement difficulty, β, is given by the ratio of the plasma pressure to the magnetic pressure and is calculated as

$$\beta = n_d \, kT/(B^2/2\mu_0), \tag{18}$$

where (3/2)kT is the average deuteron energy, B is the magnetic field strength, and μ_0 is the magnetic permeability. Even at $n_d = 10^{14}$ d^+/cm^3 in a magnetic field of 5 T, for example, β is approximately 10^{-6}. This is much less than the few percent βs achieved in conventional confinement machines. The difference is due to the much lower temperature of ions in the trapped d^+ layer of the present invention relative to the high temperatures of conventional thermonuclear plasmas. In the ICR reactor of the present invention, the target temperature can be kept low by dissipatively damping the axial motion of both the target and beam ions. The beta-limited density for 1 eV ions in a 5 T field, is 10^{20} d^+/cm^3. Thus, for equivalent ion densities, d^+ trapping in the target layer is much easier than confinement of a thermonuclear plasma.

Coulomb scattering affects both the t^+ orbits and d^+ density distribution. In the absence of electrons, this scattering is the primary energy loss mechanism for the tritons and generates the nuclear stopping discussed above. The cross-section for scattering

through an angle greater than $\theta_c/2$ is πb^2 where $\theta_c/2$ is given by Eq. (13). This cross-section varies as $1/E^2$ and is strongly peaked in the forward direction. As a result, elastic scattering of the t^+ at high energies occurs predominantly at small angles and very weakly pumps energy from the tangential motion into radial and axial modes. Initially, the Penning trap voltage V_p needs only to be sufficient to reflect the axial kinetic energy of the triton, that is, a few eV. As scattering increases this axial component, higher trapping voltages are needed. Since the t^+ energy is input only in the tangential direction, but lost equally from all directions, the fractional energy in the radial and axial modes is determined by the input and loss rates. Local density variations can be incorporated into the trap design to produce additional attenuation in specific modes. For example increased scattering or electronic attenuation near the end plates will preferentially remove higher energy longitudinal motion from the tritons. Energy can also be removed from longitudinal and radial modes by radiative damping, as is done in long life ion traps.

Elastic scattering within the low energy d^+ population will produce orbit drift, tending to form a uniform d^+ distribution across the cylinder. Since the nuclear stopping increases rapidly with decreasing energy, as shown in Figure 1, such a uniform d^+ density would cause the dominant t^+ stopping to be at low energies, corresponding to small ICR radii. Under this situation, the RF field would need to be increased to overcome this attenuation, making it too large to balance the stopping at higher energy, as desired. The rate at which this occurs depends on the d^+ density. Several ways to overcome this problem are:

(1) The higher-energy, scattered d^+ can be allowed to escape the trap at small

radii, by using a graded trapping potential $V_p(r)$ that decreases with decreasing r.

(2) Radial or cylindrical grids can be used to provide separate regions for low energy triton acceleration and deuterium sputtering. In this situation, t^+ (or scattered t^+) enters the region containing the deuterium reservoir only after reaching high energy near $r \approx R$.

(3) The d^+ density distribution can be controlled with a weak, radial logarithmic potential $+V_c$ that is applied to the cylinder axis by biasing the triton source as shown in Figure 5A. The repulsive force generated by this radial logarithmic potential can be adjusted to balance the deuteron drift produced by scattering. Using larger V_c can potentially produce very thin d^+ layers that will generate little space charge to trap electrons. A thin d^+ layer will be repelled by the reservoir surface if the surface is allowed charge positively. Such surface charging will normally result from the secondary electron emission that accompanies sputtering and can be adjusted by controlling the current to the reservoir.

Imposition of a radial logarithmic potential also stabilizes the triton orbits by generating a restoring force tending to recenter the orbit within the reactor cylinder. This can be seen by examining the change in energy occurring when an orbit is moved off-center. It is convenient to write the radial logarithmic potential as

$$V(r) = eV_c \ln(r/R)/\ln(r_c/R), \tag{19}$$

where r_c is the radius of the triton source aperture. Then, the triton's potential energy increases from zero at $r = R$ to eV_c at $r = r_c$. The derivative of V(r) is

$$\partial V(r)/\partial r = eV_c /[r\ln(r_c /R)], \quad (20)$$

which increases with decreasing r. The magnitude of V(r) increases at an increasing rate for each decrease in r. Thus, a circular orbit that traverses a spread in potentials corresponding to a spread in radial location r will have a higher average potential energy than when the orbit is centered with a single r. The magnitude of this restoring force is determined by V_c and r_c/R. Additional t^+ orbit restoring and damping forces can be designed into the trap fringe fields. This restoration is needed for accommodating the frequent orbit excursions that occur following small angle scattering. Alternatively, the tritons could be "freed" from the resonance and allowed to decelerate in a high density target region, where upon fusion energy would be generated according to $Q_{B\text{-}T}$.

DFE- 10/4/96

The condition for ion cyclotron resonance in a uniform magnetic field B(gauss) is easily formulated by balancing a circulating ion's centripetal force with the Lorentz force produced by the field. Adding an additional uniform, resonant RF field results in tangential ion acceleration and the following useful equations:

Cyclotron frequency,

$$f_0\ (Hz) = 1524(q/M)B. \quad (21)$$

Cyclotron radius,

$$r(cm) = 144.5(M^{1/2}/q)(E^{1/2}/B). \quad (22)$$

Energy increment per cycle,

$$dE/dn(eV/cy) = \pi q r E_{rf} . \quad (23)$$

DFC 10/4/96

Radial increment per cycle,

$$dr/dn(cm/cy) = 3.281 \times 10^4 (M/q)(E_{rf}/B^2). \quad (24)$$

Here q, M(amu), and E(eV) are the charge state, mass, and energy of the ion, respectively, and E_{rf}(volts/cm) is the peak RF field strength. For the curved RF plates 60 shown in Figure 5A and 5B, E_{rf} is not uniform over the cylinder and thus the ion acceleration varies during the cycle. However, for a weak RF field, the orbits remain very nearly circular and the effect produces an average E_{rf} that decreases with increasing radius by an amount depending on the angle subtended by the plates. For small plates, the decrease is a factor of two which, in turn, helps produce more rapid ion acceleration at the lower energies, further reducing elastic scattering of the accelerating ions.

DFC 10/4/96

The imposition of a logarithmic potential across the reactor affects the conditions for triton ICR. This can be seen by examining the addition of the 1/r force to the force balance equation for cyclotron motion. Use of Eq. (20) results in a quadratic equation for the cyclotron frequency with the solution

$$f(Hz) = (f_0/2) + (f_0/2)(1 - 4\gamma)^{1/2} \approx f_0 (1 - \gamma) \quad (25)$$

for small γ, where

$$\gamma = 10^8 \, V_c \, (Volts)/[2\pi f_0 \, Br^2 \ln(R/r_c)]. \qquad (26)$$

Here f_0 is the ICR frequency given by Eq. (21) in the absence of the potential. Thus, the cyclotron frequency for a concentric ion orbit is modified by a term that depends on its radius. To keep the triton in resonance throughout the reactor requires $\gamma \ll 1$, which limits V_c. Since the triton spends most of its life near radius R, the effect of this limitation is minimized if the RF frequency is tuned to the value given by Eq. (25) evaluated at $r \approx R$. With $r_c \sim 0.02R$, this frequency is shifted by less than 1 ppm/volt in a 5 T field. Near $r \approx r_c$, the shift can exceed several hundred ppm unless V_c is limited to a few volts. This off-resonance effect can be eliminated by using axial field shims 64 (Figure 5A) for tailoring the magnetic field and counterbalancing the logarithmic potential. It can be shown that the accompanying $\vec{B} \times \vec{\nabla} B$ tangential drift, that also produces a frequency shift, is two orders smaller than γ.

DFC 19/4/96

For much of the remaining discussion, a specific reactor geometry is considered for an ICR reactor using a 44 kGauss (4.4 T) solenoid. Table II lists ICR characteristics for TD, DT and ^{3}HeD reactors having a 4.4 T magnetic field. The reactors are small in size with convenient RF frequencies. The ICR frequencies for the various ions differ sufficiently to prevent acceleration of the target ions. If solid deuterium is used as a d^+ reservoir, the reservoir surface is cylindrically self-correcting in that it (and the magnet uniformity) need not be fabricated to great precision, but will assume an internal cylindrical surface that is "tuned" to the magnetic and RF field homogeneities.

TABLE II

	TD	DT	^{3}HeD
Fusion Resonance Energy, E_{Res}	200 keV	130 keV	1160 keV
Reactor/ICR Radius at E_{Res}, R	2.54 cm	1.68 cm	3.06 cm
ICR Drive Frequency, f_0	22.35 MHz	33.53 MHz	44.70 MHz
Target Ion Orbit Radius (1eV), r_t	0.0046 cm	0.0057 cm	0.0046 cm

The characteristics of a ^{3}HeD reactor are shown in Table II for comparison with TD and DT reactors. For obtaining a high Q with a ^{3}HeD reaction, the ^{3}He must be doubly ionized, meaning that $^3He^{++}$ must be the incident ion. Since the ions are resonantly accelerated, $^3He^+$ introduced on axis will not be accelerated. Rather, it will remain trapped on axis, passing repeatedly into the ionizer until becoming doubly ionized, where upon it will be accelerated.

Ion acceleration times and trapping lifetimes can be made long enough to allow the reactor of the present invention to be operated in a pulsed mode providing additional flexibility for separately optimizing trapping potentials and field shims for the acceleration and interaction phases. For example, after a number of tritons have been accelerated to the resonant energy and have begun to generate the d^+ target layer 62, the trap potentials can be changed for maximizing the ion trapping and for compressing target layer 61, 62 to a higher density. This can be done while maintaining the triton ICR condition in the interaction layer 62.

DFC 10/4/92

The net power produced by the reactor is the difference between the reaction output and the various reactor inputs,

$$P_{net} = P_{reaction\ output} - P_{triton\ input} - P_{deuteron\ layer} - P_{peripheral} . \quad (27)$$

By Eq. (17), the mean lifetime of a triton is $\tau_t = 1/[(\sigma v)_0 n_d]$. Thus, the reaction input for N_t tritons circulating at resonance is

$$P_{reaction\ output} = [(\Delta M)c^2\ ](\sigma v_t\ )_o\ n_d\ N_t\ , \quad (28)$$

The energy input to the tritons is $E_0 + 1(\sigma/s)_0$, or

$$P_{triton\ input} = (1/Q)P_{reaction\ output} . \quad (29)$$

Along with each deuteron added to the target layer, an electron is produced. The electrons generate a current to the Penning plates consuming energy. To determine this energy, consider a target layer characterized by a length L and thickness δR. If the τ_d is the mean deuteron lifetime and $N_d = (2\pi R\delta RL)n_d$ is the number of deuterons in the target layer, then the number of deuterons required per triton is $(N_d/\tau_d)(N_t/\tau_t)$. With a triton reaction rate of N_t/τ_t, the energy needed for maintaining the deuteron layer is given by

$$P_{deuteron\ layer} = eV_p\ (2\pi R\delta RLn_d\ /\tau_d). \quad (30)$$

The deuteron layer thickness used below is ten d^+ orbit diameters or $\delta R \sim 0.1$ cm. This loss is minimized by using a high magnetic field for reducing R and δR, and by minimizing the reactor length L. However, additional limits to both these dimensions also results from the effects of fringing fields on the trapping efficiency. To a first order, the lifetime τ_d is proportional to the layer volume, offsetting the apparent advantages of small dimensions.

If a solid deuterium reservoir is used, then a major peripheral energy requirement is the energy to maintain the cryogenic layer. This energy loss can be reduced by keeping the cryogenic materials thin and relatively transparent to the high-energy neutrons. The high-energy neutrons would in turn be absorbed in an outer blanket material. Under such a condition, the cryogenic heat load would then be due to the 3.5 MeV α-particles. This α-particle load actually occurs twice: Energy is lost from the output and must also be supplied at the input. The input load can be reduced by minimizing the reactor length L, thereby reducing the solid angle subtended by the cryogenic system. For a short reactor in a "pill-box" type geometry, the solid angle approaches 2π sr. Further reductions are achieved by limiting the cryogenic system to only a fraction of the circumference. The α-particle load to the end plates (or grids) can be converted directly to electrical energy or used for helping maintain the plate potential V_p. Further, the plates are not held at a low temperature. The cumulative geometric effects can be taken for providing a rough factor of two reduction in the heat load, offsetting the doubling effect. Then, this load amounts to a factor of 3.5/17.6 or 20% of the output power,

$$P_{peripheral} = 0.2P_{reaction\ output} \cdot \quad (31)$$

Using Eqs. (28)-(31) in Eq. (27) produces the output power plot shown in Figure 6. The net power produced in ICR reactor 50 is the difference between the reaction output and the various reactor inputs, including detrapping and cryogenic losses. Figure 6 is a graph showing the calculated power production for a reactor having a 2.54 cm radius and a 20 cm length with target ion densities in the range of 10^{13} - 10^{15} cm^{-3}. The abscissa of Figure 6 shows the number of tritons maintained in resonance by the RF field while the ordinate shows the output power measured in Watts. Diagonal curve families 70, 71 and 72 have a deuteron density in the target layer of 10^{13}, 10^{14} and 10^{15} cm^{-3}, respectively. The curves show that with modest ion densities, power in the watt-to-kilowatt range can be produced by a small ICR reactor.

In Figure 6, the effects of a finite average deuteron lifetime are indicated by solid symbols. An average deuteron lifetime of τ_d = 1 s are represented by solid square points 73. An average deuteron lifetime of τ_d = 0.01 s are represented by solid circle points 74. An average deuteron lifetime of τ_d = 0.0001 s are represented by solid diamond points 75. For a given deuteron density, increasing the number of tritons relaxes the requirement on deuteron lifetime. Thus, the increased deuteron detrapping, which is likely to occur at high n_d, may not necessarily present a problem. The open circular symbols 76 associated with curve family 72 shows the changes produced when the reactor length is shortened from 20 to 5 cm. Both of these effects result from the fact that a given deuteron will be burned faster if there are fewer total deuterons in the trap.

While the present invention has been described in connection with the illustrated embodiments, it will be appreciated and understood that modifications may be made without departing from the true spirit and scope of the invention.

ABSTRACT OF THE DISCLOSURE

A method and apparatus for generating nuclear fusion by ion cyclotron resonance in an ion trap reactor . The reactor includes a cylindrical housing having an axial axis, an internal surface, and first and second ends. First and second end plates that are charged are respectively located at the first and second ends of the cylindrical housing. A gas layer is adsorbed on the internal surface of the cylindrical housing. Ions are desorbed from the gas layer, forming a plasma layer adjacent to the cylindrical housing that includes first ions that have a same charge sign as the first and second end plates. A uniform magnetic field is oriented along the axial axis of the cylindrical housing. Second ions, that are unlike the first ions, but have the same charge sign, are injected into the cylindrical housing along the axial axis of the cylindrical housing. A radio frequency field resonantly accelerates the injected second ions at the cyclotron resonance frequency of the second ions. The second ions circulate in increasing helical orbits and react with the first ions, at the optimum energy for nuclear fusion. The amplitude of the radio frequency field is adjusted to accelerate the second ions at a rate equal to the rate of tangential energy loss of the second ions by nuclear scattering in the first ions, causing the ions to continually interact until fusion occurs.

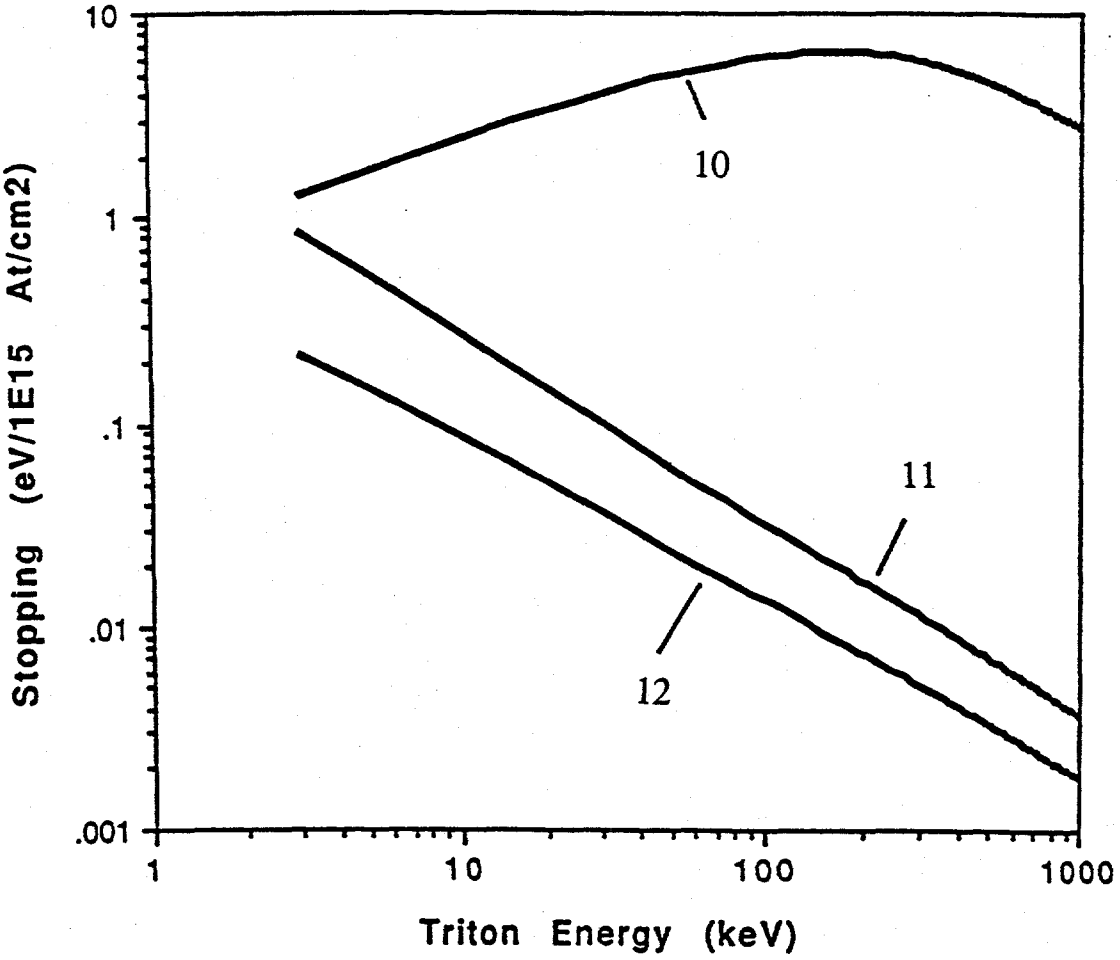
10
1
.1
.01
.001
Stopping (eV/1E15 At/cm2)
1
10
100
1000
Triton Energy (keV)
10
11
12

Fig. 1

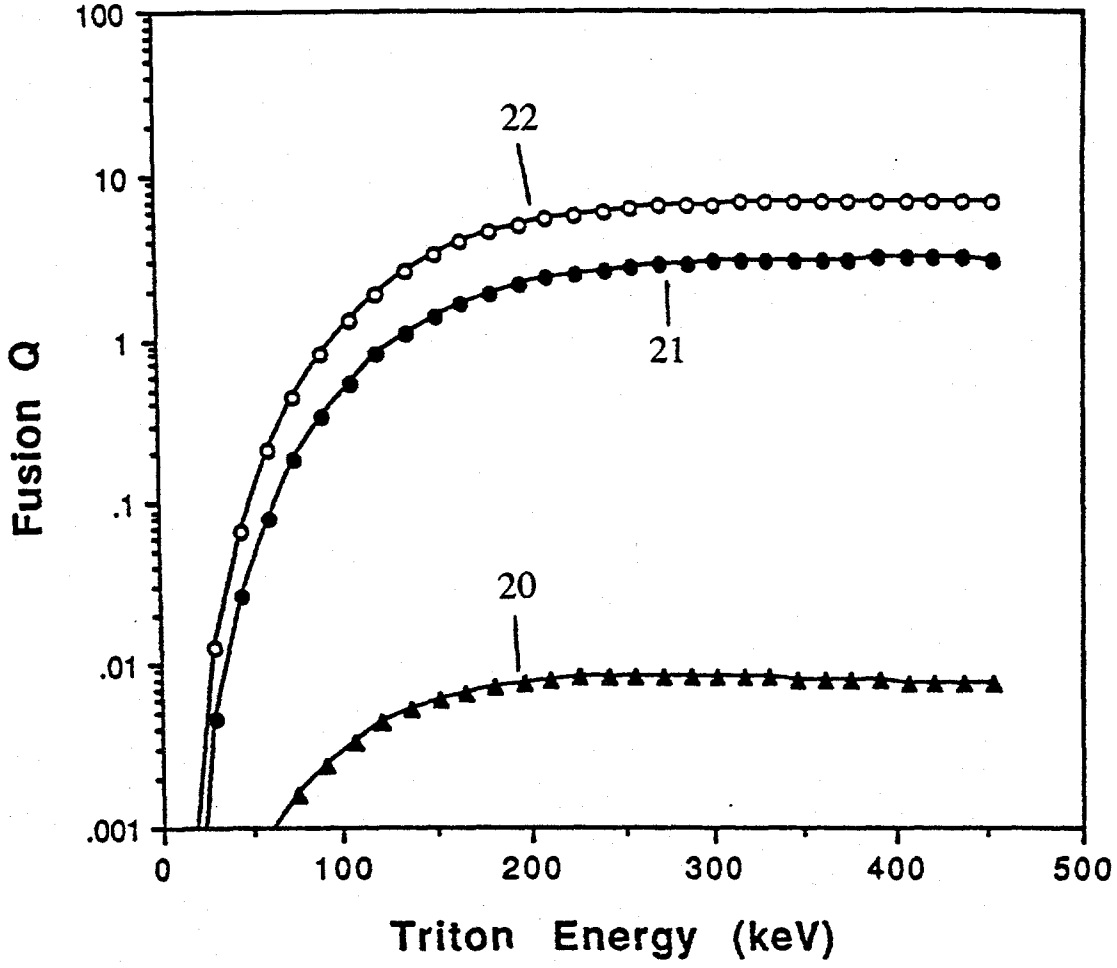
100
10
1
.1
.01
.001
Fusion Q
22
21
20
0
100
200
300
400
500
Triton Energy (keV)

Fig. 2

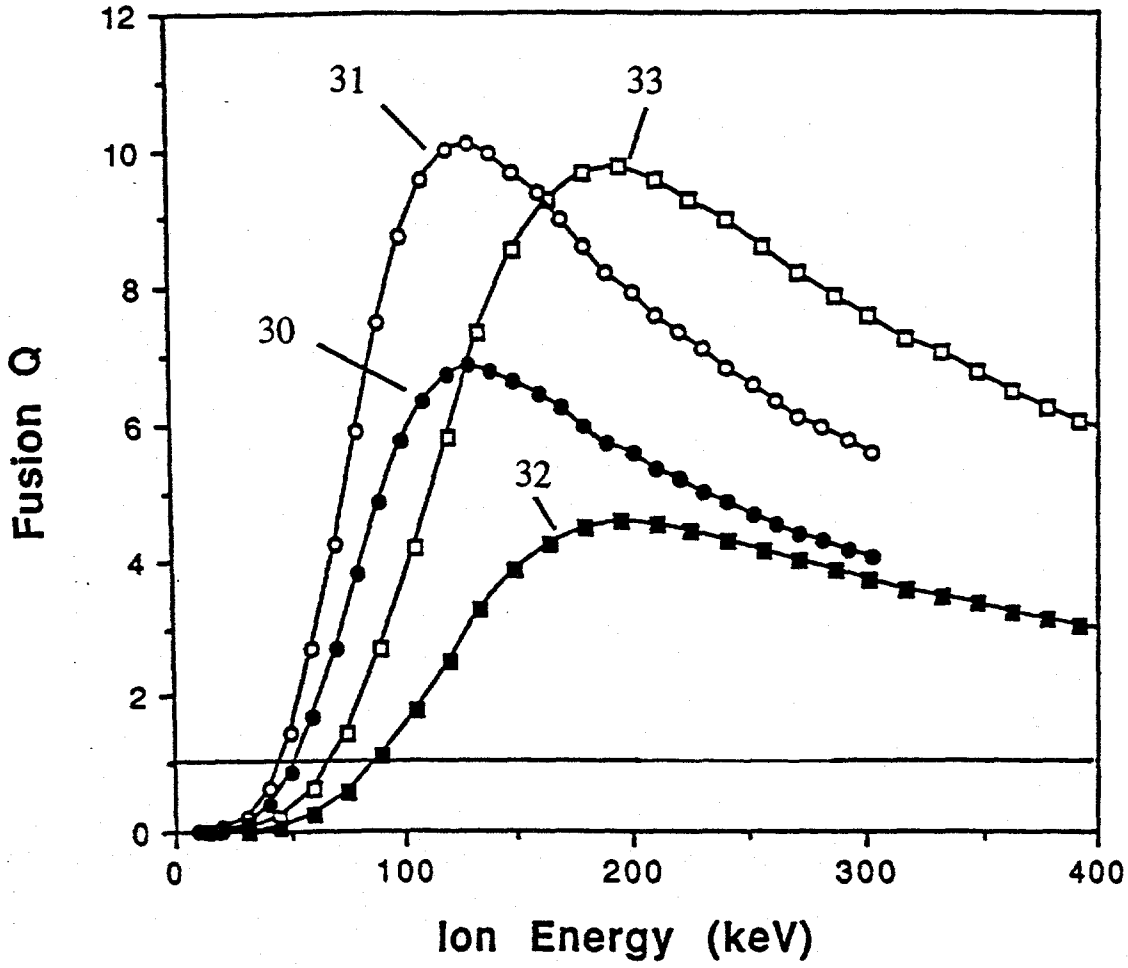

Fig. 3

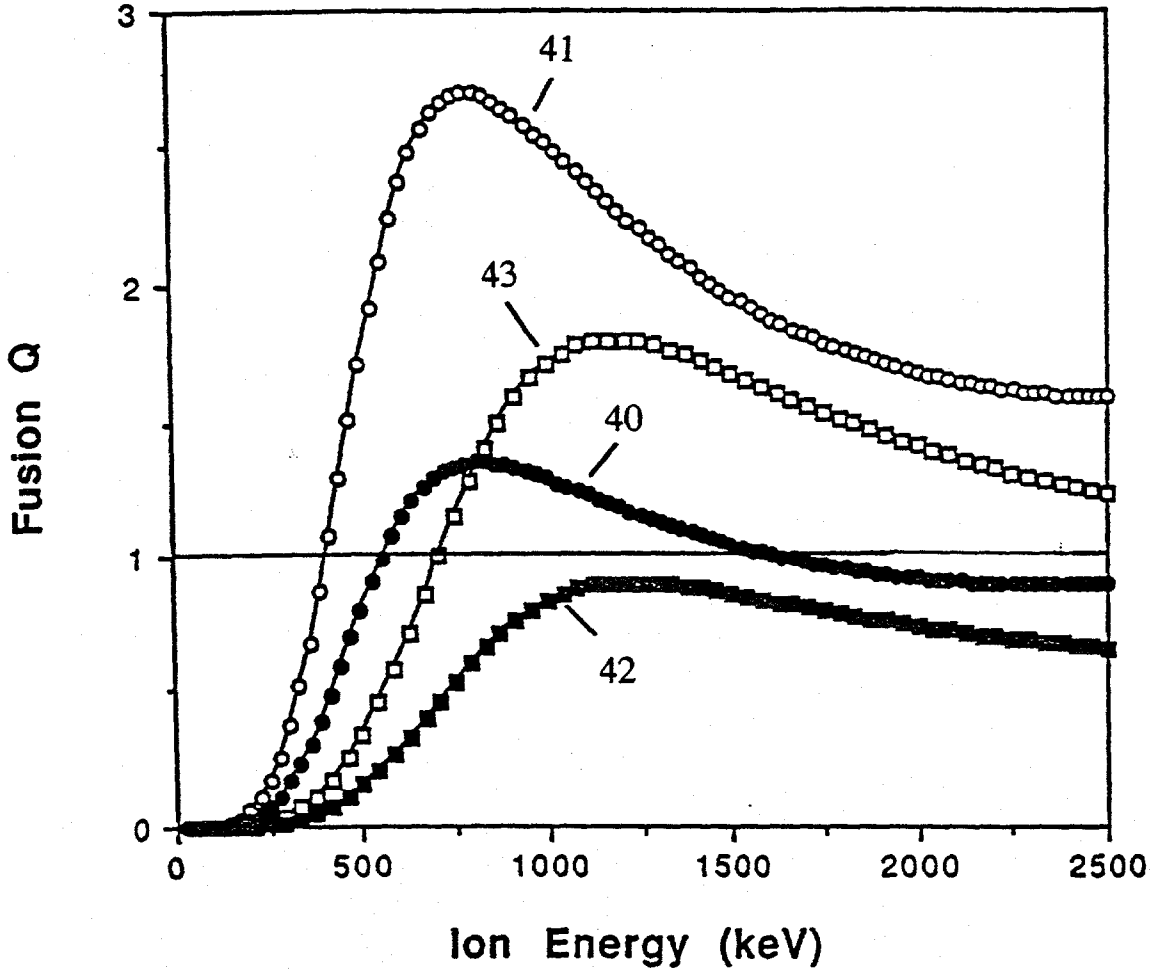
3
2
1
0
Fusion Q
41
43
40
42
0
500
1000
1500
2000
2500
Ion Energy (keV)

Fig. 4

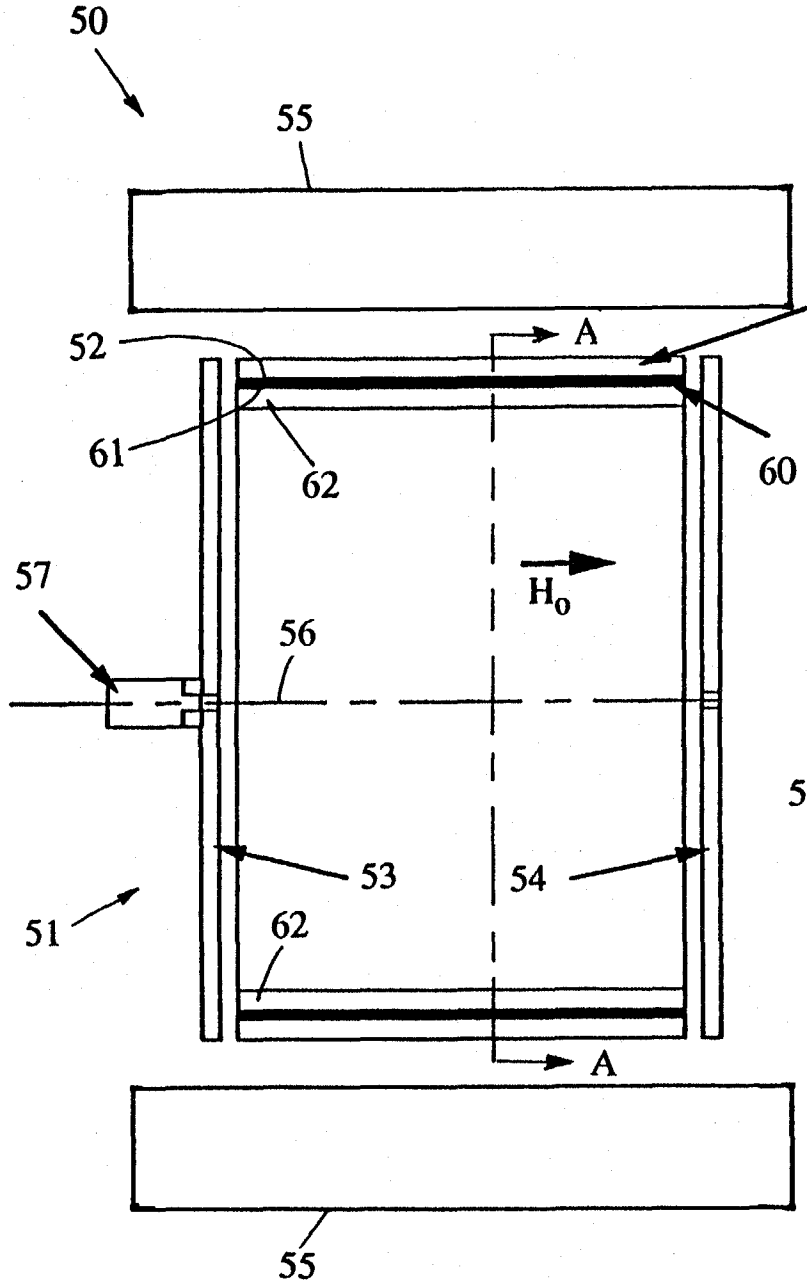

Fig. 5A

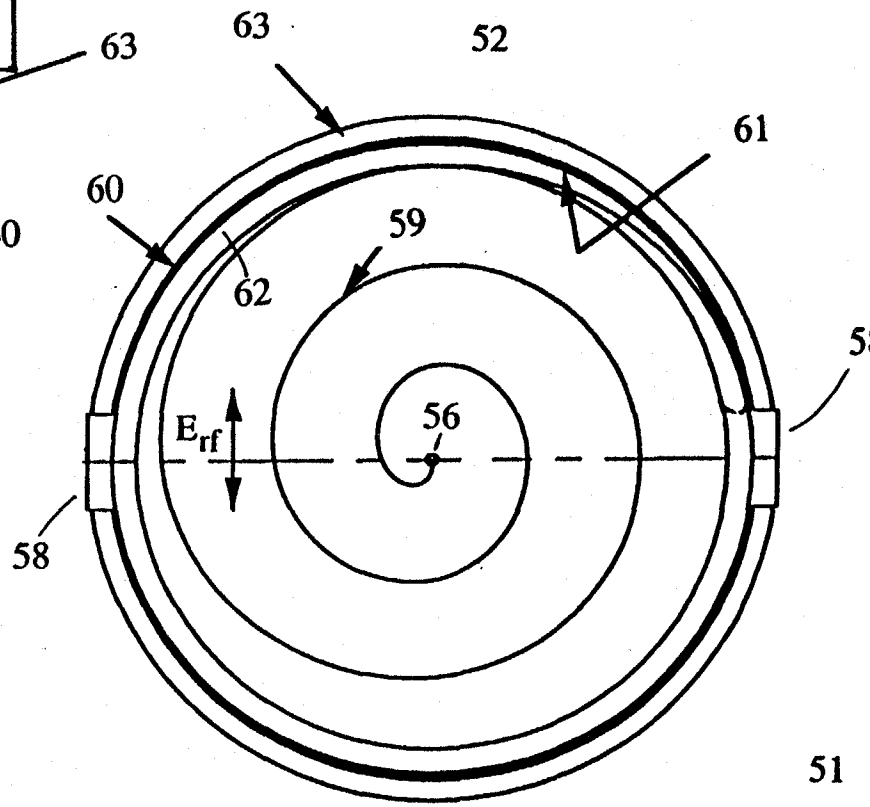

View A-A

Fig. 5B

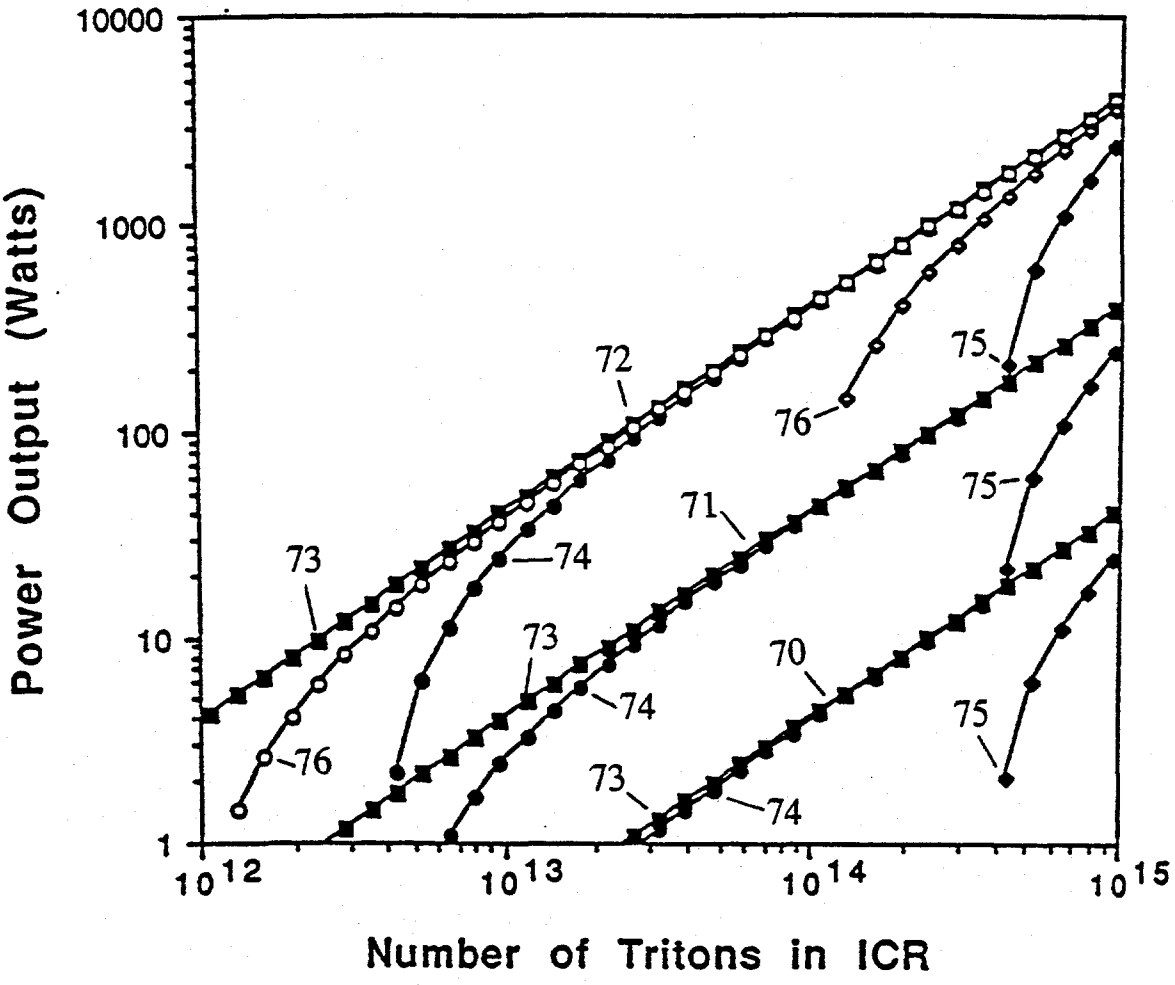
10000
1000
100
10
1
Power Output (Watts)
10^{12}
10^{13}
10^{14}
10^{15}
Number of Tritons in ICR
72
73
74
76
71
73
74
75
76
75
70
73
74
75

Fig. 6